International Scholarly Research Network
ISRN Soil Science
Volume 2012, Article ID 310927, 7 pages
doi:10.5402/2012/310927

Research Article

Within-Storm Rainfall Distribution Effect on Soil Erosion Rate

S. I. Ahmed,[1] R. P. Rudra,[1] B. Gharabaghi,[1] K. Mackenzie,[2] and W. T. Dickinson[1]

[1] *School of Engineering, University of Guelph, Albert A. Thornbrough Building, 50 Stone Road East, Guelph, ON, Canada N1G 2W1*
[2] *Golder Associates Ltd., Mississauga, ON, Canada L5N 5Z7*

Correspondence should be addressed to S. I. Ahmed, sahmed@uoguelph.ca

Received 21 February 2012; Accepted 29 April 2012

Academic Editors: G. Benckiser, L. D. Chen, A. E. M. Chirnside, J. M. Dorioz, and B. S. Sharratt

This study investigates the effect of rainfall temporal distribution pattern within a storm event on soil erosion rate and the possibility of using rain power type model for rainfall erosivity. Various rainfall distribution patterns, simulated by rainfall simulator, were used on 1.0 m^2 plot of silica sand and loam soil with a minimum of three replications. The results show that the soil erosion rates spiked following every sharp increase in rainfall intensity followed by a gradual decline to a steady erosion rate. Transient effects resulted in the soil erosion rates for an oscillatory rainfall distribution to be more than two fold higher than those obtained for a steady-state rainfall intensity event with same duration and same average rainfall intensity. The 3-parameter and 4-parameter rain power models were developed for a process-based measure of rainfall erosivity. The 4 parameter model yielded better match with the observed data and predicted soil erosion rates more accurately for silica sand under all rainfall distributions, and good results for loam soil under low intensity rainfall. More research is necessary to improve the accuracy of soil erosion prediction models for a wider range of rainfall distributions.

1. Introduction

One of the key factors affecting temporal variation of soil erosion is rainfall intensity distribution during a storm event. Many studies have been conducted at field and laboratory scale to improve the understanding of soil erosion and its relationship with rainfall amount, intensity, and pattern [1, 2]. Laboratory studies of interrill soil erosion usually employ simulated rainfall. A number of researchers have studied rainfall simulators and demonstrated the significance of various factors, including simulated raindrop size distribution, raindrop impact velocity, raindrop impact angle, and rainfall intensity and duration on rainfall erosivity [1, 3, 4]. Many rainfall simulators apply a temporally varied intensity of simulated rainfall to each small area of soil surface in a sweeping pattern [3, 5]. One potential problem with this method is that the energy flux density (power) of simulated rainfall is not always a function of the time averaged intensity [4, 6]. The power of natural rainfall has been found to be approximately linearly related to rainfall intensity [7, 8]. Meyer [4] has found that interrill detachment rates are related to the second power of intensity or more precisely as shown in

$$E = aI^{(2.1-\text{claycontent})}, \tag{1}$$

where E is the erosion rate ($\text{kg m}^{-2}\,\text{s}^{-1}$), I is the rainfall intensity (mm h^{-1}), and a is a fitted coefficient and is a function of soil type, crop cover, and other site-specific parameters. De la Rosa et al. [9] modeled erosion rates and interrill erosion for various agriculture management practices and validated interrill erosion from experimental data and found that the sediment continuity equation resulted in a good relationship between model predictions and measured interrill erosion rates.

The main objective of this study was to investigate the effect of interactions between rainfall intensities and the soil surface on interrill erosion processes. The specific objectives of this study were twofold: firstly to establish whether the rate of soil erosion depends on the temporal distribution of simulated rainfall and secondly to investigate the energy flux

Table 1: Simulated rainfall characteristics over a 1.035 m^2 plot for Spraying Systems Inc. nozzles at 1.7 m.

Spraying nozzle	System pressure (psi)	Mean intensity (mm/h)	Uniformity coefficient (%)	Rain power ($mJ\,m^2\,s^{-1}$)
1/8GGSS4.3W	7	20	82.27	45
1/4GGSS10W	10	30	90.34	68
1/4GGSS10W	7	40	73.54	91
3/8GGSS20W	5.5	110	53.16	350

density (rain power) of rainfall as a suitable parameter for quantifying rainfall erosivity.

2. Materials and Methods

This soil erosion study was performed using the Guelph Rainfall Simulator II (GRSII). GRSII was used for simulated rainfall applied in various patterns and intensities to a 1.0 m^2 plot [1, 6, 10]. The change in rainfall intensities in the subset was obtained by changing supply line pressures and nozzles. The intensities, uniformity coefficients, and powers for various Spraying Systems Inc. nozzles are shown in Table 1.

The soil flume used in this study was set at 2.9% during all rainfall runs. The soil flume also had subsurface drainage facility. The two soils used in this research were Barnes Silica Sand (39.3% sand, 45.6% silt, 15.1% clay, and 3.2% organic matter) and loam soil (39.3% sand, 45.6% silt, 15.1% clay, and 3.2% organic matter) [11].

The subsurface drains for silica sand were left open after the previous run to allow the sand to drain. The existing surface was disturbed excessively with a rake up to a depth of 50 to 60 mm to break up any existing crust or surface seal. The disturbed sand was scraped off the plot and surface was replaced with clean dry sand. The packed sand was graded down to the level of the sharp crested weir using a grader assembly. It was then rolled 20 times with the 10 kg roller. After rolling, the subsurface drain was closed and water was supplied at the height to obtain soil surface saturation. The subsurface drain was opened and the sand was allowed to drain. The soil was screened through a series of screens with a minimum opening of 2 mm. The preparation procedure used for silica sand was also applied prior to each experiment on loam.

The rainfall simulator was calibrated and each calibration run used a different nozzle and pressure setting except when repetitions were performed. Also, several qualitative observations of simulated rainfall using the modified GRSII were made during this stage.

During the experiment the eroded sand was collected in small no. 200 sieves and the mass of the eroded soil was determined by oven drying the sand collected on the sieves. For the loam soil the mass of eroded soil was determined by collecting sediment runoff from the plot in one liter Nalgene bottles on the rotating table. The volume of runoff and the concentration of sediment in the runoff were used to compute the erosion rate and runoff rate. The treatments consisted of continuous rainfall storm and intermittent storm. The continuous storms represent a natural rainstorm of short duration, and the intermittent (on-off) rainfall treatments were selected to emulate an oscillatory pattern of simulated rainfall to the soil surface. All of the rainfall treatments patterns were developed using five different simulated rainfall intensities; 0, 20, 30, 40, and 110 $mm\,h^{-1}$. Table 2 gives the details of the rainfall intensities and treatments used in this study.

Design storms that were chosen to represent short-duration natural rainstorms were stepwise in nature. All the rainfall intensities used in the storm were relatively low compared to natural rainfall. The initial 33.3% duration of the storm had a constantly applied 32 $mm\,h^{-1}$ followed by 40 $mm\,h^{-1}$ intensity for the next 33.3% duration and 20 $mm\,h^{-1}$ for the last 33.3% of the duration. For silica sand experiments, the duration of each intensity was 20 min for a whole storm duration of 60 min (SVC). For the loam soil experiments, the duration of each intensity in the rainfall distribution was 15 min for a whole storm duration of 45 min (LVC). The sequence of simulated rainfall intensities was the same as the rainfall distribution on silica sand.

For the silica sand experiments the on-off rainfall treatment was one hour in duration with six replications (S15) for the first on-off cycle. For the loam soil experiment, the on-off rainfall treatment was 45 min long with three replications (L15). This was primarily due to limitations on the number of samples that could be rapidly processed.

A second on-off cycle (30 seconds) treatment of 40 $mm\,h^{-1}$ intensity of simulated rainfall was applied to both soils (S30 and L30 for sand and loam, resp.). The third on-off treatment, applied to each soil (S67 and L67 for sand and loam, resp.), was rainfall application with an intensity of 110 $mm\,h^{-1}$. Rainfall was applied for 15 seconds followed by a 67-second off cycle.

For the comparison purposes, a control treatment of constant 20 $mm\,h^{-1}$ intensity of rainfall was also applied to sand (CS) and loam (CL) soils. The erosion and runoff data generated from these treatments were converted into the erosion rate (ER) ($mg\,m^{-2}\,s^{-1}$) and the integral of erosion rate or total erosion. Further analyses were attempted to relate these variables to the rate of dissipation of rainfall kinetic energy at the surface or Rain Power, P ($mJ\,m^{-2}\,s^{-1}$). This term is also called the energy flux density by Tossell et al. [6, 10].

Valmis et al. [12] investigated the importance of water stability and its relationship to soil aggregation and interrill erosion. The results permitted classification of soils with respect to water stability of aggregates and consequently

Table 2: Details of various treatments for the study.

Soil type	Treatment	Instantaneous rainfall intensity (mm/h)	Rainfall pattern	Mean rainfall intensity (mm/h)
Sand	SVC	32-40-20	Continuous for 60 min, 20 min each	30
	CS	20	Continuous for 60 min	20
	S15	40	15 s off and 15 s on for 60 min	20
	S30	40	30 s off and 30 s on for 60 min	20
	S67	110	15 s on and 67 s off for 60 min	20
Loam	LVC	30-40-20	Continuous for 45 min, 15 min each	30
	CL	20	Continuous for 45 min	20
	L15	40	15 s off and 15 s on for 45 min	20
	L30	40	30 s off and 30 s on for 45 min	20
	L67	110	15 s on and 67 s off for 45 min	20

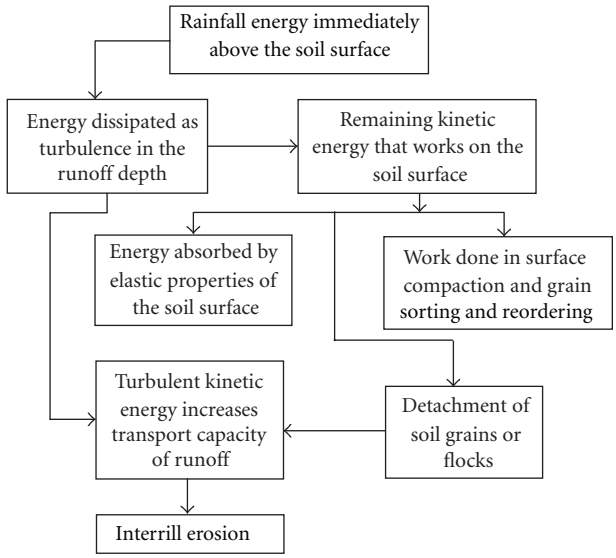

Figure 1: An illustration of the processes that describe the energy based model for interrill erosion for this study.

allowed interrill erosion to be expressed as a function of an instability index. They showed that the stability index fluctuated temporally and proposed that the instability index was an easier parameter to measure then the interrill erodibility term.

A theoretical energy-based model of the interrill erosion process was proposed for this study. A schematic of this model is shown in Figure 1. For natural rainfall a similar more empirical model could be developed based on the intensity of rainfall rather than the rain power. It is expected that this model could perform as well as the rain power model because of the close linear relationship between the energy and intensity of natural rainfall. The interrill detachment process is thought to begin with the kinetic energy of raindrops immediately before impacting the soil surface. The energy of all drops impacting a surface is often described in terms of a distribution and termed as the energy flux density or rain power ($\mathrm{mJ\,m^{-2}\,s^{-1}}$). When rainfall impacts a layer of runoff, some of its energy is dissipated as the drop shears through the layer of runoff [13, 14]. It has been demonstrated that the shear across the surface between the impacting drop and the runoff layer spawns small, short-lived, and local bursts of intense turbulence [15–18].

The energy remaining after penetrating the runoff depth is dissipated doing work on the soil surface. The work done on the soil surface can be sorted into three main categories. First is the energy that is dissipated elastically by the soil surface. The second is surface compaction and grain ordering or armouring often lumped together and termed crusting. The third is detachment where raindrops work to detach soil flocs and grains from the soil surface. Once detached grains move downslope and become eroded interrill soil provided that the transport capacity of the runoff depth is not limiting. The Reynolds number calculated using bulk flow variables is laminar for most interrill flows [19]. The transport capacity of runoff is largely governed by rain drop impact.

2.1. Rain Power Models. The proposed model for interrill detachment is similar to the models suggested by Sharma and Gupta model [20] for single-drop detachment and to Meyer [4] for interrill detachment model. The main difference in (2) is the inclusion of the work terms to describe the transient behavior of the soil surface during a storm:

$$D = d\left[a(P - P_0)^b + \frac{C}{W + W_a}\right], \tag{2}$$

where D is the detachment rate ($\mathrm{mg\,m^{-2}\,s^{-1}}$), P is the rain power ($\mathrm{mJ\,m^{-2}\,s^{-1}}$), P_0 is the critical power that can be absorbed elastically or without detaching soil ($\mathrm{mJ\,m^{-2}\,s^{-1}}$), W is the work done on the surface at any time since the onset of rainfall ($\mathrm{mJ\,m^{-2}}$), W_a quantifies the antecedent condition of the soil crust ($\mathrm{mJ\,m^{-2}}$), a, b, c, and d are fit coefficients, and P_0 and W_a are found by fitting to a data set. The procedure for estimating P_0 is the same as that presented by Bagnold [21]. The coefficient "d" in (2) is thought to represent the fraction of rainfall power remaining after penetrating the runoff depth. In reality, this parameter is nearly impossible

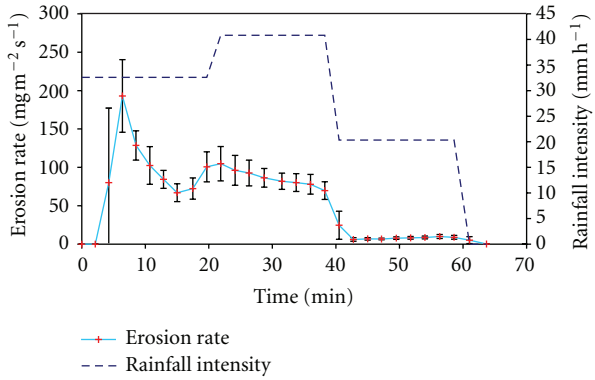

Figure 2: Average erosion rate under three rainfall intensities of 32-40-20 mm/hr for silica sand. The error bars show ±1 standard deviation.

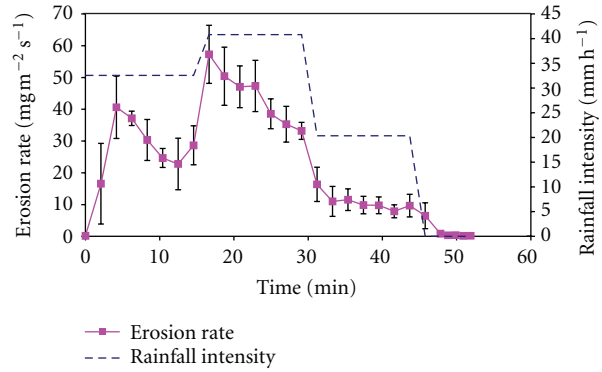

Figure 3: Average erosion rate under three rainfall intensities of 32-40-20 mm/hr for loam soil. The error bars show ±1 standard deviation.

to quantify and can easily be included in the coefficients "a" and "c" to yield the following:

$$D = a(P - P_0)^b + \frac{C}{W + W_a}. \quad (3)$$

Equation (3) is referred to as the four parameters model in this study. The three-parameter model is a simplification of (3), wherein the P_0 term is assumed equal to zero. The data collected in this research was not sufficient to determine W. Therefore, this parameter was approximated as the integral of rain power since the onset of rainfall. This approximation embeds significant empiricism into the second term in (2) and (3). In (3), the parameter "a" can be indexed as a soil erodibility parameter. The coefficient "c" is related to the crustability of the soil surface. A soil that behaves very differently from its disturbed state when it is fully crusted will have a large value for "c". This can be due to its compactability, swelling clay content, uniformity, or grain isotropy (armouring). It is recommended that the parameter W_a be dropped from (3) when the soil surface has been recently disturbed as is often the case in laboratory studies. Furthermore, the last term in (3) can be dropped when the soil is already well crusted, that is, W_a is very large. This latter case may occur in field conditions many months after tilling.

Qualitative observations of trends in the data support the inclusion of the critical power term P_0. The effect of this parameter is evident at low rainfall intensities after full crust formation. This parameter partially describes the discrepancies in erosion rates observed between experiments under continuous rainfall and under temporally varied rainfall. When the difference $P - P_0$ is less than or equal to zero the detachment rate will approach zero because the rainfall energy is distributed and occasional drops, in the tail of the distribution, may still acquire sufficient energy to detach.

3. Results

The average soil erosion rate for the simulated storm that was applied to sand and loam (Figures 2 and 3) shows a distinct dependence on the rainfall intensity and hence rain power for silica sand. Initially, up to 4 minutes the erosion rate is zero despite the application of 32 mm h^{-1} rainfall (Figure 3). Then erosion rate started to increase and erosion rate was affected by a transient condition, which may be described by two possible hypotheses. Firstly, the sand detached from the surface during the 6 min prior to full runoff can be considered to be loose on the surface because of the noncohesive nature of this soil. Upon commencement of runoff, this loose sand begins to be delivered to the outflow at the transport capacity rate of the flow. Secondly, the soil surface prior to the storm is in a disordered and uncompacted state despite the surface preparation. At the onset of rainfall, the surface has little capacity to resist erosion. The formation of surface armoring gradually increases the strength of the sand and, hence, its ability to resist erosion. Both of these hypotheses are supported by the observation of a gradual decline in erosion rate until about 24 minutes of this simulated storm have passed. After 24 minutes, the change in erosion rate with time (Figure 1) is relatively steady; this could be due to the soil surface tending toward its final condition under rainfall, that is, a fully crusted condition. The gradual decay in the erosion rate toward its steady state-rate (for each rainfall intensity) appears to follow an exponential or hyperbolic pattern which could be described as the integration of rain power.

Figure 3 shows the results of LVC treatment on loam soil. These data show that the trends are similar in nature to the similar treatments on silica sand but differ in the magnitude of erosion rate. Also, the data for loam soil show more scatter than those from silica sand. This is primarily attributed to less control over the antecedent soil moisture conditions and the collection mechanism. Due to less runoff, eroded sand was collected in its entirety while eroded loam was sampled from a large volume of water. These data also show that the transient part of the erosion rate consists of an initial climb to a high erosion rate followed by decaying to some steady value. The initial high rate of erosion coincides with the occurrence of full and steady runoff generated by 32 mm h^{-1} rainfall intensity at about 5 min. Since loam is a relatively cohesive soil, it is more reasonable to attribute the reduction

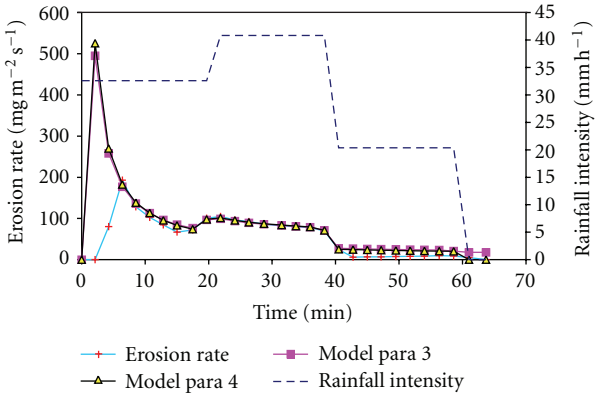

Figure 4: Comparison of observed and predicted erosion rate under three rainfall intensities of 32-40-20 mm/hr for silica sand.

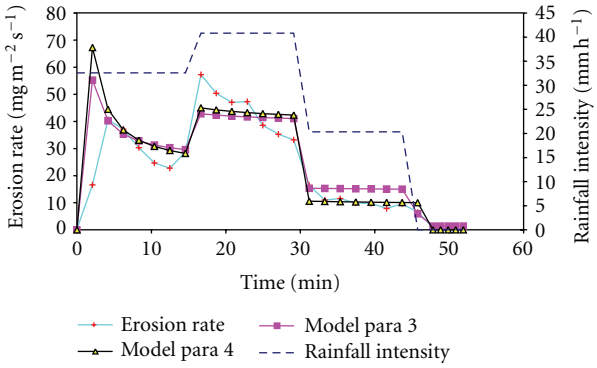

Figure 5: Average erosion rate from silica sand under constant 20 mm h^{-1} rainfall. The error bars show ±1 standard deviation.

in erosion rate entirely to crusting processes rather than to the loose soil hypothesis. The transient part of the erosion rate response of LVC (Figure 3) again seems to follow an exponential or hyperbolic decay similar to SVC (Figure 2).

The gradual increase in erosion rate after the step down to 20 mm h^{-1} rainfall intensity is not seen in LVC (Figure 3). This could be due to the different settling characteristics of silica sand and loam. Therefore, it is reasonable to deduce that the transport capacity of the runoff layer was larger than the detachment rate occurring as a result of rainfall impact for loam soil. In the case of silica sand for the same treatment, it is likely that the detachment rate was close to or even higher than the capacity transport rate.

Further, the erosion rates for SVC and LVC were compared with the proposed detachment model (3) (Figures 4 and 5). The predictions of the detachment model depict that both the 3- and 4-parameter models performed well when compared with the observed erosion rates from both soils. However, these models overpredicted the erosion rates in the beginning of the storm (0 to 7 min) for both soils. Overall, these models predicted better for sand than the loam soil (Table 3). These data show that the value of P_0 is more than double for sand when compared with the value for loam soil. This may be a consequence of the similar initial treatment of the two soils before each experiment or a function of the

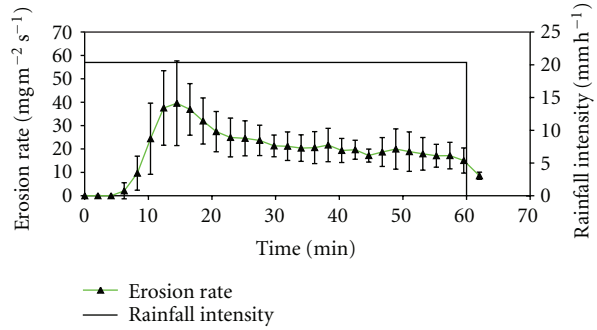

Figure 6: Comparison of observed and predicted erosion rate under three rainfall intensities of 32-40-20 mm/hr for loam.

Table 3: Best fit coefficients for detachment model and goodness of fit criteria for silica sand and loam.

Soil	a	b	c	P_0
Sand	4.6×10^{-5}	3.4	3.9×10^{6}	19.1
Loam	6.0×10^{-2}	1.5	3.2×10^{5}	8.7

interaction between the drop size distribution and the soil surface. These data also show that parameter "b" varies with soil type, indicating that the cohesive soil is more resistant to the erosive forces of rainfall.

3.1. Control Treatment. Figures 6 and 7 show the observed erosion rate under continuous and constant rainfall intensity of 20 mm h^{-1} (control) rainfall for sand and loam, respectively. These data show that for silica sand (Figure 6) the erosion rate is zero. As soon as runoff begins after 5 min, the erosion rate increases significantly which could be due to the uncrusted initial conditions at the sand surface. The initial high erosion rate is followed by a gradual decay to the steady state erosion rate. This transient response lasts approximately 35 min, and the steady state erosion rate persists till the end of rainfall event. For constant application of rainfall at an intensity of 20 mm h^{-1} on sand the steady erosion rate was about 15 mg m^{-2} s^{-1}. The data for loam soil (Figure 7) show that the change in observed erosion rate is similar to silica sand.

3.2. On-Off Rainfall Storm. Figure 8 shows the observed erosion rates for treatments S15, S30, and S67 for silica sand. The data for S15 treatment showed an initially low erosion rate (12.9 mg m^{-2} s^{-1}) followed by a sharp increase to a peak erosion rate (90.9 mg m^{-2} s^{-1}) and then a gradual decay to the steady state erosion rate. The steady erosion rate was approximately 33 mg m^{-2} s^{-1}, roughly twice the rate observed under CS treatment (Table 4). The increase is attributed to the increased instantaneous rainfall intensity during the S15 treatment.

The result for S30 treatment on silica sand also shows trends similar to S15 treatment (Figure 8). The erosion rates for S67 also depict similar characteristic response to other treatments. The steady erosion rate under this rainfall treatment was about 20 mg m^{-2} s^{-1} (Table 4), less than the

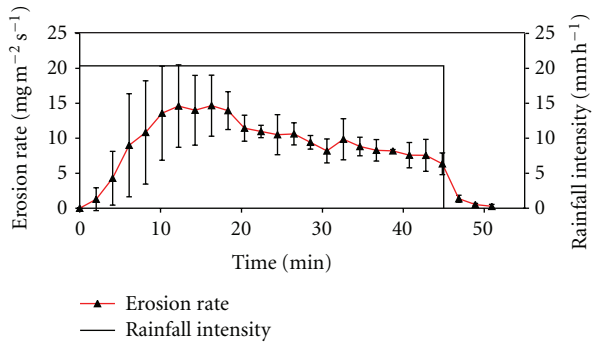

Figure 7: Average erosion rate from loam under constant 20 mm h^{-1} rainfall. The error bars show ±1 standard deviation.

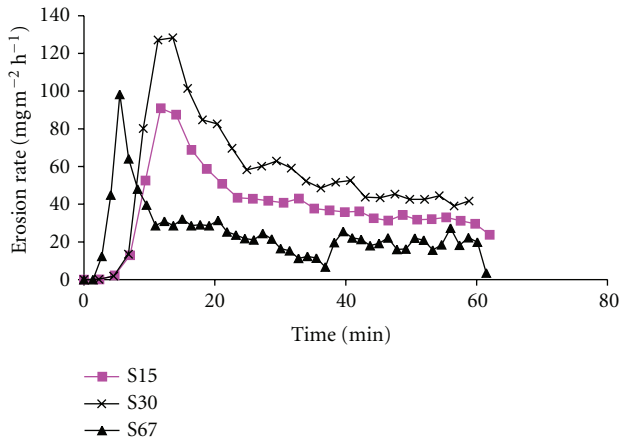

Figure 8: Erosion rates from silica sand under three different rainfall patterns: S15 = 40 mm h^{-1} at 15 s ON and 15 s OFF; S30 = 40 mm h^{-1} at 30 s ON and 30 s OFF; S67 = 110 mm h^{-1} at 15 s ON and 67 s OFF.

Table 4: Summary of trends in erosion rates under on and off rainfall applications.

Treatment	Time to peak (min)	Peak erosion rate (mg m^{-2} s^{-1})	Mean erosion rate (mg m^{-2} s^{-1})
CS	15	39	15
S15	13	91	33
S30	14	128	43
S67	6	98	20
CL	16	15	8
L15	6	48	17
L30	6	53	17
L67	13	91	35

S15 and S30 treatments as might be expected. This may be due to the lack of transport capacity during a 67-second long pulse of off cycle.

Figure 9 shows the trend of loam soil erosion rate was similar to silica sand, namely, the initially low erosion rate followed by a sharp increase to a peak erosion rate then a gradual decay to the steady state-rate of erosion. However, these observations indicate that erosion rates from loam are

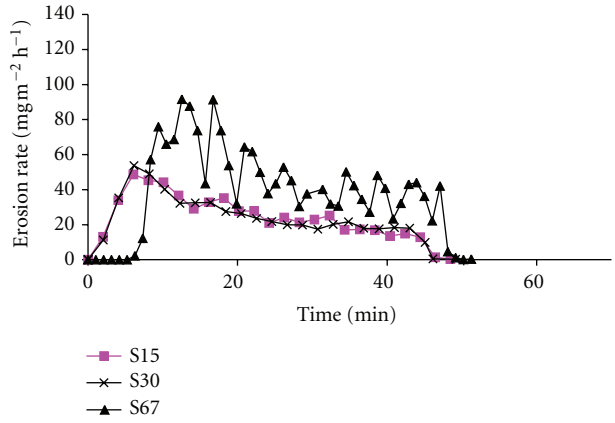

Figure 9: Erosion rates from loam under three different rainfall pattern: S15 = 40 mm h^{-1} at 15 s ON and 15 s OFF; S30 = 40 mm h^{-1} at 30 s ON and 30 s OFF; S67 = 110 mm h^{-1} at 15 s ON and 67 s OFF.

dominated by detachment rate which is governed by the rainfall intensity and are less affected by transport capacity rates. Conversely, for the silica sand the reduced transport capacity during off cycles has a significant effect on erosion rates because more energy is required to transport the coarser sand particles.

Overall, for both the soils the erosion rates increased with an increase in on cycle rainfall intensity with the exception of the S67 treatment for silica sand. Reduced erosion rate for the S67 treatment is because runoff depth during off cycles became too shallow to actively transport detached sediment. This scenario would allow for rapid deposition of previously detached sediment.

4. Conclusions

The study to evaluate the effect of rainfall pattern on soil erosion showed that within-storm rainfall distribution has an important effect on soil erosion rate. The observed average erosion rates for sand and loam under variable rainfall intensity were significantly higher than the erosion rates for sand and loam under constant rainfall intensity for the same duration. It was also observed that the soil erosion rates spiked following every sharp increase in rainfall intensity followed by a gradual decline to a steady erosion rate. These transient effects resulted in the soil erosion rates for an oscillatory rainfall distribution to be more than twofold higher than the soil erosion rate for a steady-state rainfall intensity event with the same duration and the same average rainfall intensity for both soil types.

The study also concluded that the rainfall energy flux density (rain power) models provided fairly accurate measurements of rainfall erosivity when compared with the observed data. It shows that the modeling framework developed in this study has potential for studying the rain power and erosion relationship; however, further work is necessary on the application of "rain power" as a measure of rainfall erosivity for different rainfall patterns and durations to improve the accuracy of soil erosion prediction models

to a wider range of soil types and rainfall intensities. Also, the findings of this study and more research in this direction will be helpful in applying the best management practices to control erosion for various hydrologic and soil conditions.

References

[1] R. W. Tossell, W. T. Dickinson, R. P. Rudra, and G. J. Wall, "A portable rainfall simulator," *Canadian Agricultural Engineering*, vol. 29, no. 2, pp. 155–162, 1987.

[2] C. C. Truman, T. C. Strickland, T. L. Potter, D. H. Franklin, D. D. Bosch, and C. W. Bednarz, "Variable rainfall intensity and tillage effects on runoff, sediment, and carbon losses from a loamy sand under simulated rainfall," *Journal of Environmental Quality*, vol. 36, no. 5, pp. 1495–1502, 2007.

[3] R. M. Bajracharya, W. J. Elliot, and R. Lal, "Interrill erodibility of some Ohio soils based on field rainfall simulation," *Soil Science Society of America Journal*, vol. 56, no. 1, pp. 267–272, 1992.

[4] L. D. Meyer, "Rainfall simulators for soil conservation research," *Soil Erosion Research Methods*, pp. 75–96, 1988.

[5] A. M. Liebenow, W. J. Elliot, J. M. Laflen, and K. D. Kohl, "Interrill erodibility. Collection and analysis of data from cropland soils," *Transactions of the American Society of Agricultural Engineers*, vol. 33, no. 6, pp. 1882–1888, 1990.

[6] R. W. Tossell, G. J. Wall, R. P. Rudra, W. T. Dickinson, and P. H. Groenevelt, "The Guelph rainfall simulator II: part 2—a comparison of natural and simulated rainfall characteristics," *Canadian Agricultural Engineering*, vol. 32, no. 2, pp. 215–223, 1990.

[7] P. I. A. Kinnell, "The problem of assessing the erosive power of rainfall from meteorological observations," *Proceedings of Soil Science Society America Journal*, vol. 37, no. 4, pp. 617–621, 1973.

[8] W. H. Wischmeier and D. D. Smith, "Rainfall energy and its relationship to soil loss," *Transactions of the American Geophysics Union*, vol. 39, no. 2, pp. 285–291, 1958.

[9] D. De la Rosa, E. Diaz-Pereira, F. Mayol et al., "Raindrop impact stress and the breakdown of soil crumbs," *Journal of Soil Science*, vol. 28, pp. 247–258, 1977.

[10] R. W. Tossell, G. J. Wall, R. P. Rudra, W. T. Dickinson, and P. H. Groenevelt, "The Guelph rainfall simulator II: part 1—simulated rainfall characteristics," *Canadian Agricultural Engineering*, vol. 32, no. 2, pp. 205–213, 1990.

[11] Agriculture Canada, "Vessie site survey and soil laboratory analysis," Unpublished internal records, Guelph Ontario, Canada, 1990.

[12] S. Valmis, D. Dimoyiannis, and N. G. Danalatos, "Assessing interrill erosion rate from soil aggregate instability index, rainfall intensity and slope angle on cultivated soils in central Greece," *Soil and Tillage Research*, vol. 80, no. 1-2, pp. 139–147, 2005.

[13] J. M. Gregory, "Physically based simple erosion theory," *American Society of Agricultural Engineers*, 1984, Paper no. 84-2547, St. Joseph, Mich, USA.

[14] L. O. Owoputi, *A physically based study of the mechanism of sediment detachment in the soil erosion process [Unpublished Ph.D. Dissertation]*, University of Saskatchewan, Saskatoon, Canada, 1994.

[15] H. H. Ghadiri and D. Payne, "Raindrop impact stress and the breakdownof soil crumbs," *Journal of Soil Science*, vol. 28, pp. 247–258, 1977.

[16] H. H. Ghadiri and D. Payne, "Raindrop impact stress," *Journal of Soil Science*, vol. 32, no. 1, pp. 41–49, 1981.

[17] H. H. Ghadiri and D. Payne, "The formation and characteristics of splash following raindrop impact on soil," *Journal of Soil Science*, vol. 39, no. 4, pp. 563–575, 1988.

[18] M. A. Nearing, L. D. Norton, D. A. Bulgakov, G. A. Larionov, L. T. West, and K. M. Dontsova, "Hydraulics and erosion in eroding rills," *Water Resources Research*, vol. 33, no. 4, pp. 865–876, 1997.

[19] B. T. Guy, W. T. Dickinson, and R. P. Rudra, "The roles of rainfall and runoff in the sediment transport capacity of interrill flow," *Transactions of the American Society of Agricultural Engineers*, vol. 30, no. 5, pp. 1378–1386, 1987.

[20] P. P. Sharma and S. C. Gupta, "Sand detachment by single raindrops of varying kinetic energy and momentum," *Soil Science Society of America Journal*, vol. 53, no. 4, pp. 1005–1010, 1989.

[21] R. A. Bagnold, "Bed load transport by natural rivers," *Water Resources Research*, vol. 13, no. 2, pp. 303–312, 1977.